ANL/ET/CP-82379
Conf-9404137--1

Nonlinear Dynamics of Tube Arrays in Cross Flow*

S. S. Chen, Y. Cai, and S. Zhu

Energy Technology Division
Argonne National Laboratory
Argonne, Illinois 60439, USA.

DISCLAIMER

This report was prepared as an account of work sponsored by an agency of the United States Government. Neither the United States Government nor any agency thereof, nor any of their employees, makes any warranty, express or implied, or assumes any legal liability or responsibility for the accuracy, completeness, or usefulness of any information, apparatus, product, or process disclosed, or represents that its use would not infringe privately owned rights. Reference herein to any specific commercial product, process, or service by trade name, trademark, manufacturer, or otherwise does not necessarily constitute or imply its endorsement, recommendation, or favoring by the United States Government or any agency thereof. The views and opinions of authors expressed herein do not necessarily state or reflect those of the United States Government or any agency thereof.

The submitted manuscript has been authored by a contractor of the U. S. Government under contract No. W-31-109-ENG-38. Accordingly, the U. S. Government retains a nonexclusive, royalty-free license to publish or reproduce the published form of this contribution, or allow others to do so, for U. S. Government purposes.

RECEIVED
APR 18 1994
OSTI

For presentation at the Twelfth Symposium on Energy Engineering Sciences, April 27-29, 1994, Argonne, IL.

*This work was funded by the U.S. Department of Energy, Office of Basic Energy Sciences, Division of Engineering and Geosciences, under Contract W-31-109-Eng-38.

MASTER

DISTRIBUTION OF THIS DOCUMENT IS UNLIMITED

NONLINEAR DYNAMICS OF TUBE ARRAYS IN CROSS FLOW

S. S. Chen, Y. Cai, and S. Zhu

Energy Technology Division
Argonne National Laboratory
Argonne, Illinois 60439, USA.

ABSTRACT

Fluidelastic instability of loosely supported tube arrays was studied analytically and experimentally. This is one of the important practical problems of autonomous fluid-structure systems with many interesting motions. Both fluid-damping and fluid-stiffness controlled instabilities were investigated. Depending on the system parameters, the dynamic response of the tubes includes periodic, quasiperiodic, and chaotic motions. The analytical model is based on the unsteady flow theory, which can predict the nonlinear dynamics of tube arrays in cross flow. For fluid-damping controlled instability, analytical results and experimental data agree reasonably well.

1. INTRODUCTION

A group of circular tube submerged in cross flow can be subjected to dynamic instability, typically referred to as fluidelastic instability. The threshold flow velocity at which tubes begin to undergo large oscillations is called the critical flow velocity (see Fig. 1). If a system component is operated at a flow velocity above the critical value, severe damage to the components is likely to occur, often after only a short time of operation. In fact, fluidelastic instability of tube arrays in cross flow has been one of the main mechanisms causing tube failure in heat exchangers and steam generators [1-3]. Since the early 1970s, extensive studies of fluidelastic instability have been reported. A significant understanding of the problem now exists. However, at present, it is still not possible to predict instability phenomena from fundamental principles of fluid dynamics and the theory of elasticity. This paper is to present an integrated experimental and analytical study with an emphasis to characterize the nonlinear dynamics of fluidelastic instability of loosely supported tube arrays. It includes:

- The unsteady flow theory of fluidelastic instability of tube arrays.
- Experiment of fluid-damping controlled instability.
- A theory of fluid-damping controlled instability.
- Analysis of fluid-stiffness controlled instability.

Analytical and experimental results show the existence of chaotic, quasiperiodic, and periodic motions when the flow velocity exceeds the critical flow velocity for loosely supported tube arrays in cross flow.

2. UNSTEADY FLOW THEORY FOR FLUIDELASTIC INSTABILITY OF TUBE ARRAYS

Consider a group of n identical tubes with radius R (= D/2) subjected to cross flow as shown in Fig. 2. The variables associated with the tube motion in the x and y directions are flexural rigidity EI, tube mass per unit length, m, structural damping coefficient C_s, and displacement u_j and v_j. The equations of motion for tube j in the x and y directions are [2,4]:

$$EI\frac{\partial^4 u_j}{\partial z^4}+C_s\frac{\partial u_j}{\partial t}+m\frac{\partial^2 u_j}{\partial t^2}+\sum_{k=1}^{n}\rho\pi R^2\left(\alpha_{jk}\frac{\partial^2 u_k}{\partial t^2}+\sigma_{jk}\frac{\partial^2 v_k}{\partial t^2}\right)+\sum_{k=1}^{n}\left(\frac{\rho U^2}{\omega}\alpha'_{jk}\frac{\partial u_k}{\partial t}+\frac{\rho U^2}{\omega}\sigma'_{jk}\frac{\partial v_k}{\partial t}\right)+\sum_{k=1}^{n}\rho U^2\left(\alpha''_{jk}u_k+\sigma''_{jk}v_k\right)=0 \tag{1}$$

$$EI\frac{\partial^4 v_j}{\partial z^4}+C_s\frac{\partial v_j}{\partial t}+m\frac{\partial^2 v_j}{\partial t^2}+\sum_{k=1}^{n}\rho\pi R^2\left(\tau_{jk}\frac{\partial^2 u_k}{\partial t^2}+\beta_{jk}\frac{\partial^2 v_k}{\partial t^2}\right)+\sum_{k=1}^{n}\left(\frac{\rho U^2}{\omega}\tau'_{jk}\frac{\partial u_k}{\partial t}+\frac{\rho U^2}{\omega}\beta'_{jk}\frac{\partial v_k}{\partial t}\right)+\sum_{k=1}^{n}\rho U^2\left(\tau''_{jk}u_k+\beta''_{jk}\right)=0 \tag{2}$$

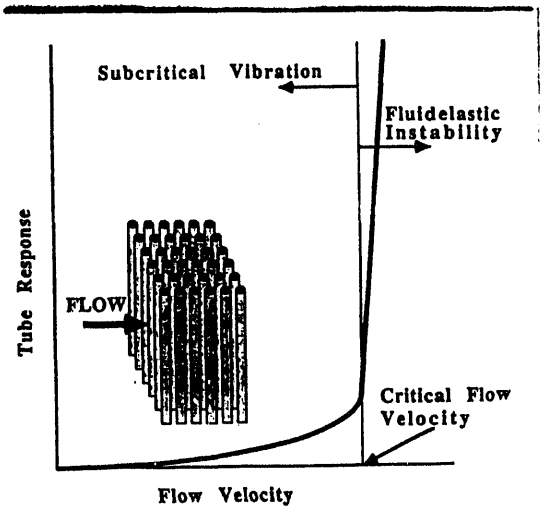

Figure 1. Response of tube arrays in crossflow

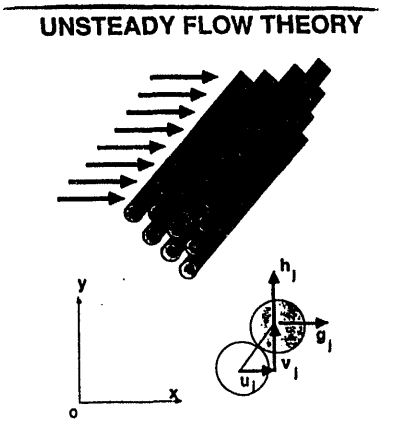

Figure 2. Tube displacements and fluid forces

where t is time; ρ is fluid density; U is flow velocity; ω is circular frequency of oscillations; α_{jk}, σ_{jk}, τ_{jk}, and β_{jk} are added mass coefficients; α'_{jk}, σ'_{jk}, τ'_{jk}, and β'_{jk} are fluid-damping coefficients; and α''_{jk}, σ''_{jk}, τ''_{jk}, and β''_{jk} are fluid-stiffness coefficients. Note that fluid-damping coefficients and fluid-stiffness coefficients are functions of reduced flow velocity U_r (= $U/f_f D$; f_f is the oscillation frequency of the tubes in flow).

The in-vacuum variables are mass per unit length m, modal damping ratio ζ_v and natural frequency f_v (= $\omega_v/2\pi$). The values for f_v and ζ_v can be calculated from the equation of motion and appropriate boundary conditions or from tests in vacuum (practically in air). The modal function of the tube vibrating in vacuum and in fluid is $\psi(z)$;

$$\frac{1}{\ell}\int_0^1 \psi^2(z)dz = 1 \tag{3}$$

where ℓ is the length of the tubes. Let

$$u_j(z,t) = a_j(t)\psi(z), \qquad v_j(z,t) = b_j(t)\psi(z) \tag{4}$$

where $a_j(t)$ and $b_j(t)$ are functions of time only. Using Eqs. 3 and 4, calculation of Eqs. 1 and 2 yields

$$\frac{d^2a_j}{dt^2} + 2\zeta_v\omega_v\frac{da_j}{dt} + \omega_v^2 a_j + \frac{\rho\pi R^2}{m}\sum_{k=1}^{n}\left(\alpha_{jk}\frac{d^2a_k}{dt^2} + \sigma_{jk}\frac{d^2b_k}{dt^2}\right) - \frac{\rho U^2}{m\omega}\sum_{k=1}^{n}\left(\alpha'_{jk}\frac{da_k}{dt} + \sigma'_{jk}\frac{db_k}{dt}\right) - \frac{\rho U^2}{m}\sum_{k=1}^{n}\left(\alpha''_{jk}a_k + \sigma''_{jk}b_k\right) = 0 \tag{5}$$

$$\frac{d^2b_j}{dt^2} + 2\zeta_v\omega_v\frac{db_j}{dt} + \omega_v^2 b_j + \frac{\rho\pi R^2}{m}\sum_{k=1}^{n}\left(\tau_{jk}\frac{d^2a_k}{dt^2} + \sigma_{jk}\frac{d^2b_k}{dt^2}\right) - \frac{\rho U^2}{m\omega}\sum_{k=1}^{n}\left(\tau'_{jk}\frac{da_k}{dt} + \beta'_{jk}\frac{db_k}{dt}\right) - \frac{\rho U^2}{m}\sum_{k=1}^{n}\left(\tau''_{jk}a_k + \beta''_{jk}b_k\right) = 0 \tag{6}$$

when the dimensionless parameters are

$$U_v = \frac{U}{f_v D}, \qquad \gamma = \frac{\rho\pi R^2}{m}. \tag{7}$$

Equations 5 and 6 become

$$\ddot{a}_j + \gamma \sum_{k=1}^{n} \left(\alpha_{jk}\ddot{a}_k + \sigma_{jk}\ddot{b}_k\right) + 2\zeta_v\omega_v\dot{a}_j - \frac{\gamma}{\pi^3}U_v^2\left(\frac{\omega_v^2}{\omega}\right)\sum_{k=1}^{n}\left(\alpha'_{jk}\dot{a}_k + \sigma'_{jk}\dot{b}_k\right)$$
$$+\omega_v a_j - \frac{\gamma}{\pi^3}U_v^2\omega_v^2\sum_{k=1}^{n}\left(\alpha''_{jk}a_k + \sigma''_{jk}b_k\right) = 0 \tag{8}$$

$$\ddot{b}_j + \gamma \sum_{k=1}^{n} \left(\tau_{jk}\ddot{a}_k + \beta_{jk}\ddot{b}_k\right) + 2\zeta_v\omega_v\dot{b}_j - \frac{\gamma}{\pi^3}U_v^2\left(\frac{\omega_v^2}{\omega}\right)\sum_{k=1}^{n}\left(\tau'_{jk}\dot{a}_k + \beta'_{jk}\dot{b}_k\right)$$
$$+\omega_v^2 b_j - \frac{\gamma}{\pi^3}U_v^2\omega_v^2\sum_{k=1}^{n}\left(\tau''_{jk}a_k + \beta''_{jk}b_k\right) = 0 \tag{9}$$

where the dot denotes differentiation with respect to t.

Once the fluid-force coefficients are known, it is straightforward to analyze the stability of a tube array in crossflow. Equations 8 and 9 can be written

$$[M]\{\ddot{Q}\} + [C]\{\dot{Q}\} + [K]\{Q\} = \{0\}, \tag{10}$$

or

$$[M_s + M_f]\{\ddot{Q}\} + [C_s + C_f]\{\dot{Q}\} + [K_s + K_f]\{Q\} = \{0\}, \tag{11}$$

where $\{Q\}$ is the displacement vectors consisting of a_j and b_j; $[M]$ is the mass matrix, including structural mass $[M_s]$ and added mass $[M_f]$; $[C]$ is the damping matrix, including structural damping $[C_s]$ and fluid damping $[C_f]$; and $[K]$ is the stiffness matrix, including structural stiffness $[K_s]$ and fluid stiffness $[K_f]$.

Fluidelastic instability of tube arrays are caused by high-velocity flow; its effects are contained in the matrices $[C_f]$ and $[K_f]$. These matrices are functions of fluid-damping and fluid-stiffness coefficients. Different types of dynamic instability can be classified according to the dominant terms in Eq. 11.

Fluid-Damping Controlled Instability (Single-Mode Flutter): The dominant terms are associated with the symmetric part of the damping matrix $[C_f]$. The instability arises because the fluid-dynamic forces create negative damping. α'_{jj} and β'_{jj} play the most important role in determining the stability-instability boundaries.

Fluid-Stiffness-Controlled Instability (Coupled-Mode Flutter): The dominant terms are associated with the antisymmetric part of the stiffness matrix $[K_f]$. It is called coupled-mode flutter, because a minimum of two modes are required to produce it. In this case, α''_{jk} and τ''_{jk} for j \o=,/) k play the major role in determining the stability characteristics.

3. MOTION-DEPENDENT FLUID FORCES

Several experiments focused on measuring motion-dependent fluid forces directly. Teh and Goyder [5] measured fluid forces acting on a tube that was excited to oscillation. These fluid forces were related to the oscillating tube only; therefore, they can be used for fluid-damping-controlled instability only. Hara [6] measured unsteady fluid forces acting on a tube row and studied the detailed flow field. Funakawa et al. [7] performed an experimental study of unsteady fluid forces acting on tube arrays with a pitch ratio of 1.41 in two-phase flow. However, these authors only measured a single component of the fluid forces for a specific motion. The results provide some insights into the instability of tube arrays in two-phase flow but cannot be used for practical prediction of instability. The most extensive measurements of motion-dependent fluid forces were by Tanaka [8]; Tanaka and Takahara [9]; and Tanaka, Takahara, and Ohta [10], who measured motion-dependent fluid forces for tube rows and square arrays with pitch ratios of 1.33 and 1.42. This technique was also used by Jendrzejczyk and Chen [11].

In this study, we used the unsteady flow theory. Fluid-force coefficients can be determined by measuring the fluid forces acting on the tubes that are due to oscillations of a particular tube. For example, if tube k is excited in the y direction, its displacement in the y direction is given by

$$v_k = v\cos\omega t. \tag{12}$$

The fluid force acting on tube j in the x direction can be written

$$f_j = \frac{1}{2}\rho U^2 c_{jk}\cos\left(\omega t + \phi_{jk}\right)v, \tag{13}$$

where c_{jk} is the fluid-force amplitude and ϕ_{jk} is the phase angle by which the fluid force acting on tube j leads the displacement of tube k. In the analytical model, the fluid force f_j is given by

$$f_j = -\rho\pi R^2\sigma_{jk}\frac{\partial^2 v_k}{\partial t^2} + \frac{\rho U^2}{\omega}\sigma'_{jk}\frac{\partial v_k}{\partial t} + \rho U^2\sigma''_{jk}v_k. \tag{14}$$

With Eqs. 12 and 14, we can also write the fluid-force component as

$$f_j = \left(\rho\pi R^2\omega^2\sigma_{jk} + \rho U^2\sigma''_{jk}\right)v\cos\omega t - \rho U^2\sigma'_{jk}v\sin\omega t. \tag{15}$$

Combining Eqs. 13 and 15 yields

$$\sigma''_{jk} = \frac{1}{2}c_{jk}\cos\phi_{jk} - \frac{\pi^3}{U_r^2}\sigma_{jk} \tag{16}$$

and

$$\sigma'_{jk} = \frac{1}{2}c_{jk}\sin\phi_{jk}, \tag{17}$$

where U_r is the reduced flow velocity ($U_r = \pi U/\omega R$).

The added mass coefficient σ_{jk} in Eq. 16 can be calculated by applying the potential-flow theory [2,12]. Then σ'_{jk} and σ''_{jk} can be calculated from Eqs. 16 and 17, when the force amplitude c_{jk} and phase angle ϕ_{jk} are measured. Other fluid-force coefficients can be obtained in the same manner.

Fluid-force coefficients depend on tube arrangement, tube pitch, oscillation amplitude, oscillation frequency, and flow velocity. For a given tube array, fluid-force coefficients are a function of oscillation amplitude (d/D) and reduced flow velocity (U_r), where d is vibration amplitude and D is tube diameter. For small-amplitude oscillations, fluid-force coefficients can be considered a function of reduced flow velocity only.

Tests in a water channel for different tube arrays have been performed to obtain fluid-damping and fluid-stiffness coefficients: a single tube, two tubes, and tube rows. The detailed test section, force transducer, test procedure, and experimental data are given in reports and papers [13-15?].

4. EXPERIMENTAL STUDY OF FLUID-DAMPING CONTROLLED INSTABILITY

Heat exchanger tubes are typically supported by tube support plates (TSP) at intervals along their length. To facilitate assembly and relative motion caused by thermal expansion, TSP holes are made larger than the tube diameter. This experiment is to evaluate the effects of tube to TSP clearance on tube motion in water flow. The experiments are performed in a rectangular flow channel that is 26.04 cm high and 10.6 cm wide and is situated in a test chamber connected to a water loop with a maximum flow rate of 0.052 m^3/s. The details of the test chamber are the same as those in earlier experiments for tube arrays in crossflow [16-18?].

The arrangement of the tube array is shown in Fig. 3. It is a tube row or square tube array with the pitch-to-diameter ratio equal to 1.35. Each tube element is suspended as a simply supported beam on two O-rings mounted 91.4 cm (36 in.) apart (A to D). The O-rings are seated in compression plates. The tube is submerged in fluid between the two O-ring supports (A to D) but is subjected to flow only in its middle portion B to C (measuring 26.04 cm). Two types of tubes are used:

- The tube at the center in the upstream row, marked by darker color in Fig. 3, called active tube, is a brass tube with 1.59 cm OD, 1.59 mm wall thickness, and 126.52 cm length.
- All other tubes are brass tubes, called dummy tubes, with 1.59 cm OD, 0.32 cm wall thickness, 95.25 cm length.

The overhung portion (the portion outside the tube support A and D) for the dummy tubes is 1.91 cm, and for the active tube is 1.91 cm at one end and 33.34 cm at the other end. The overhung portion of the active tube between D and G is in air.

The active tube is also "supported" by a brass TSP. Two types of TSP are used: rectangular shape and circular shape. The diametral clearance (gap) between the tube and the TSP is set at different values to study the effect of clearance on tube response. Displacement transducers at a and b are used to measure tube displacement.

Tube displacements at a and b in the lift and drag directions are recorded on tape. The tube response can be observed at the overhung portion; in particular, interaction of the free end with the TSP can be seen when the flow velocity is changed. The tube displacement components are analyzed in detail to provide an understanding of the response characteristics; these include RMS tube displacements, time histories, power spectral densities, dominant response frequencies, phase planes, Poincaré maps, and Lyapunov exponents. Figures 4-6 show typical tube response characteristics as a function of flow velocity including rms displacement, phase planes, and Lyapunov exponent. Tube displacements associated with the instability of a TSP-inactive mode are small; however, impacts of the tube against TSPs may result in significant damage in a relatively short time. The detailed data of three series of tests are presented in a report [17].

5. A THEORY FOR FLUID-DAMPING CONTROLLED INSTABILITY

The tube motion for the tube row given in Figure 3 is analyzed based on the unsteady flow theory. Several techniques, including rms tube displacements, bifurcation diagrams, phase portraits, power spectral density, and Poincaré mapping, are used to characterize tube motions. Many calculations have been carried out to thoroughly confirm the existence of chaotic motion and the routes to chaos with change of control parameters [19?].

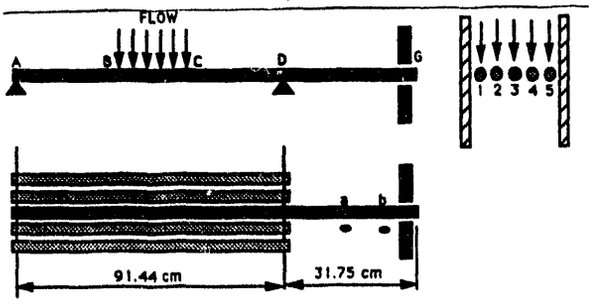

Figure 3. Schematic of a square array

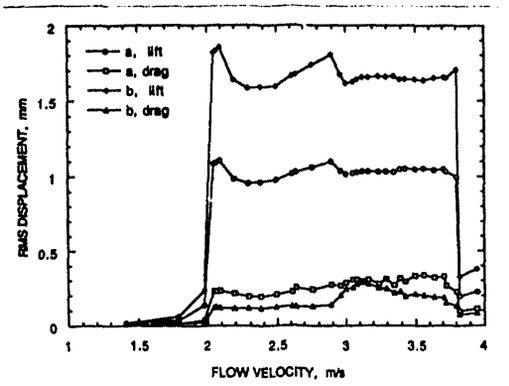

Fig. 4. RMS tube displacement as a function of flow velocity

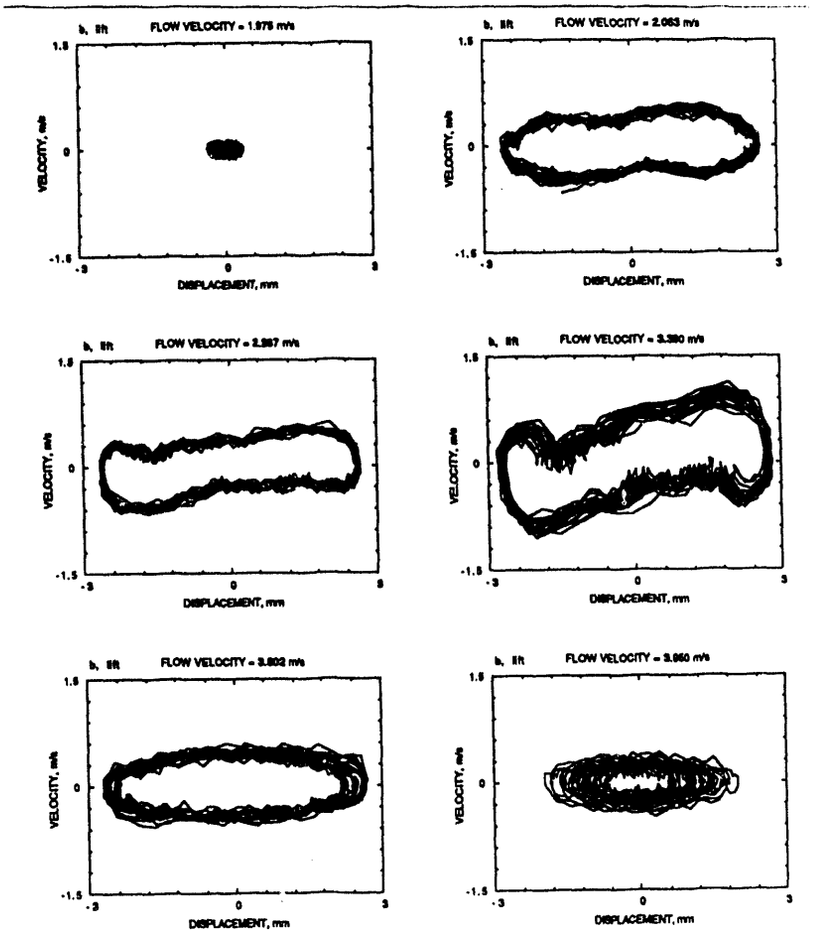

Figure 5. Phase planes of displacement transducer b

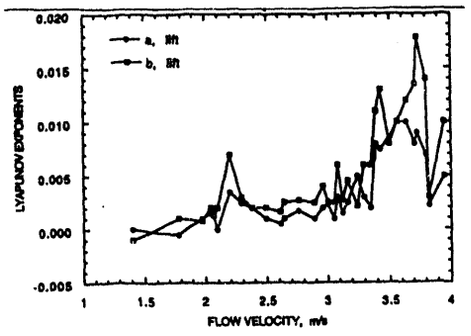

Figure 6. Lyapunov exponent as a function of flow velocity

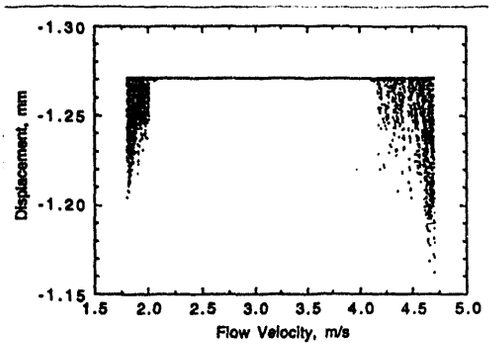

Figure 7. Bifurcation diagram

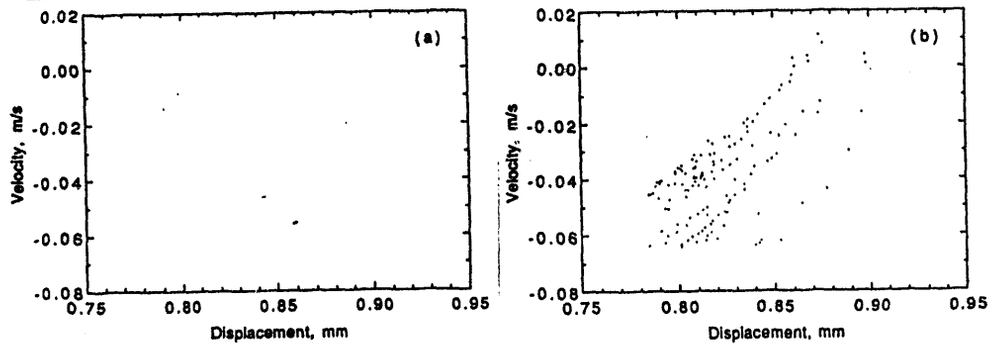

Figure 8. Poincaré map of tube motion at (a) 2.1 m/s and (b) 2.0 m/s

Figure 7 shows the bifurcation diagram for a symmetric clearance. For flow velocity less than the first critical flow velocity 1.77 m/s or higher than the second critical flow velocity 4.73 m/s, all oscillations died out as time increased; when flow velocity reached the critical values, there was a jump in displacement. When the tube lost its stability and struck the TSP, chaotic motion occurred. But as flow velocity reached certain values between 2.02 m/s and 4.17 m/s, the tube struck the TSP regularly in a harmonic periodic vibration because of the damping-controlled instability of the tube.

Figure 8 shows the Poincaré map of tube motion at 2.1 and 2.0 m/s. Figure 8a presents periodic motion because there is only a single point. However, Figure 8b shows limited-band chaotic motion with points scattered over a wide range.

Figure 9 shows the RMS displacement predicted from the mathematical model and derived from experimental data. The lower and upper limits of critical flow velocity are in good agreement. Predicted tube displacement at b, which is close to the TSP, agree well with the experimental data. The predicted response at b is slightly lower than that in the experimental data.

Based on an unsteady-flow theory and a bilinear mathematical model, fluidelastic instability of loosely supported tubes subjected to crossflow was analyzed. With typical nonlinear boundary conditions, tube motion can be expressed by a nonlinear autonomous mechanical system in which chaotic motion is highly probable with variation of control parameters. In this study, a very complicated system was analyzed using 10 modes. Therefore, the chaotic behavior of the system may be quite different from systems with one or two-degrees-of-freedom. Even though the analytical results in this study demonstrated the existence and identified some characteristics of chaotic motion in the instability region of the TSP-inactive mode, we still have difficulties with completely understanding why the chaotic motion occurs and how we can control it economically.

6. ANALYSIS OF FLUID-STIFFNESS CONTROLLED INSTABILITY

The system consists of a row of rigid tubes with three tubes supported by springs, as shown in Fig. 10. The middle three tubes are denoted as tubes 2, 1, and 3 respectively. The coupled tube/flow system consists of six degrees of freedom; three elastically supported tubes have two degrees of freedom each. The openings on the support plate are assumed to be squares with tube support plate gaps, a_j, b_j, c_j, and d_j.

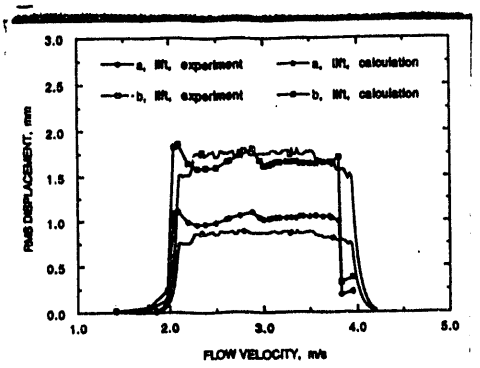

Figure 9. Comparison of theoretical results and exponent data of RMS tube displacements

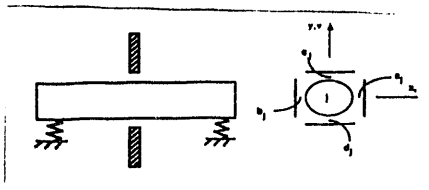

Figure 10. Rigid tubes supported by springs and gaps between tubes and support plates

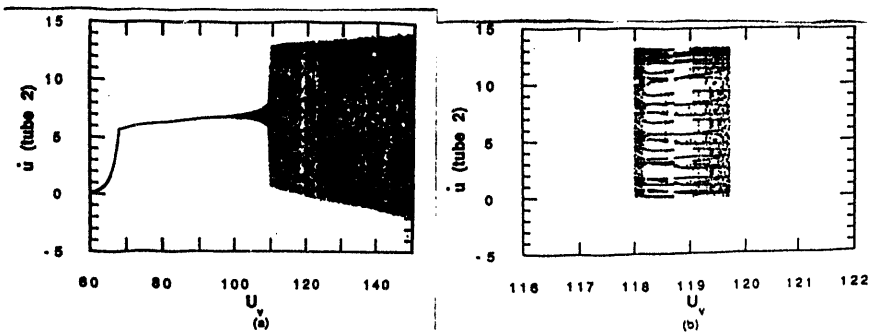

Figure 11. Bifurcation diagram

An analysis using time simulations, power spectral densities, bifurcation diagrams, Poincaré maps, and Lyapunov exponents has been performed to investigate the motions of a row of loosely supported tubes in crossflow. This is the first study on chaotic vibration associated with stiffness-controlled instability of loosely supported tubes on the basis of the unsteady flow theory.

Figure 11 shows the bifurcation diagram, in which U_V is slowly increased to observe the change of dynamic behavior. The u axis is the velocity of tube 2 whenever tube 1 passes through the equilibrium position. In the area above the second Hopf Bifurcation, a number of periodic windows is visible.

For a range of system parameters, flow-induced instability is periodic with a single frequency. The periodic motion can become chaotic through one or more of the following ways: (1) the reduced flow velocity is increased until the second Hopf Bifurcation occurs, (2) the gap is asymmetric, and (3) the gaps for one tube are larger than those for other tubes. The detailed results are given in two papers [20, 21?].

7. CLOSING REMARKS

Fluidelastic instability of loosely supported tube arrays was studied analytically and experimentally. Both fluid-damping and fluid-stiffness controlled instabilities were investigated. The nonlinearity of the symmetric or asymmetric gaps significantly affects the distribution of periodic, quasiperiodic, and chaotic motions of the tubes. This is one of the practical problems of fluid-structure systems with many interest motions.

To develop a reliable design guideline for fluidelastic instability of tube arrays for application to heat exchangers and steam generators, the unsteady flow theory is the reliable theory to use. The key elements are the motion-dependent fluid force coefficients. In this study, a reliable method was developed and shown capable of providing all necessary fluid force coefficients. A systematic study can be performed to measure all fluid force coefficients for various tube arrays. Once the necessary fluid force coefficients are determined, the unsteady flow theory can be applied to practical components for the evaluation of fluidelastic instability.

Several series of tests were performed for a loosely supported tube among a rigid tube array in crossflow. Tube displacements were analyzed to characterize the tube behavior by RMS values, power spectral densities, phase planes, Poincaré maps,

and Lyapunov exponents. The general characteristics predicted from the mathematical model based on the unsteady flow theory agree reasonably well with experimental data.

Continuing work will emphasize the development of a basic understanding of fluid/structure systems, either autonomous or nonautonomous. Nonlinear models based on the unsteady-flow theory will be developed to establish the basis for appropriate stability control techniques. The research will be directed to focus on some basic question: (1) what are the nonlinear characteristics of motion-dependent fluid forces? (2) What causes the hysteresis associated fluidelastic instability? (3) Under what circumstances is flow instability a necessary condition for fluidelastic instability? (4) How does vortex shedding interact with fluidelastic instability? (5) How does turbulence excitation affect fluidelastic instability? (6) What are the useful applications of fluidelastic instability? (7) What is the best technique to control chaos in fluid/structure systems.

ACKNOWLEDGMENTS

This work was funded by the U.S. Department of Energy, Office of Basic Energy Sciences, Division of Engineering and Geosciences, under Contract W-31-109-Eng-38.

REFERENCES

1. Paidoussis, M. P., 1980, "Flow-Induced Vibrations in Nuclear Reactors and Heat Exchangers," In Practical Experiences with Flow-Induced Vibration, Ed. E. Naudascher and D. Rockwell, pp. 1-81, Springer Verlag.
2. Chen, S. S., 1987, "Flow-Induced Vibration of Circular Cylindrical Structures," Hemisphere Publishing Corp., New York.
3. Axisa, F., 1993, "Flow-Induced Vibration of Nuclear System Components," In Technology for the '90s, ASME Publication, pp. 897-956.
4. Chen, S. S., 1989, "Some Issues Concerning Fluidelastic Instability of a Group of Circular Cylinders in Crossflow," J. Pressure Vessel Technology, Vol. 111, pp. 507-518.
5. Teh, C. E., and H. G. D. Goyder, 1988, "Data for the Fluidelastic Instability of Heat Exchanger Tube Bundles," In Flow-Induced Vibration and Noise in Cylinder Arrays, ASME Publication, New York, pp. 77-94.
6. Hara, F., 1987, "Unsteady Fluid Dynamic Forces Acting on a Single Row of Cylinders Vibrating in a Cross Flow," In Flow-Induced Vibrations-1987, Ed. M. K. Au-Yang and S. S. Chen, PVP-Vol. 122, pp. 51-58.
7. Funakawa, H., T. Tshimatsu, K. Kumon, and T. Ochiai, 1990, "Vibration of Tube Arrays Induced by Two-Phase Normal Flow," JSME Int. J., Series III, Vol. 33, pp. 483-487.
8. Tanaka, H., 1980, "Study on Fluidelastic Vibration of Tube Bundle," Nihon Kikai Gakkai Ronbunshu, or Japan Soc. Mech. Eng., Section B, Vol. 46, pp. 1398-1407.
9. Tanaka, H., and S. Takahara, 1981, "Fluid Elastic Vibration of Tube Array in Cross Flow," J. Sound Vib., Vol. 77, pp. 19-37.
10. Tanaka, H., S. Takahara, and K. Ohta, 1982, "Flow-Induced Vibration of Tube Arrays with Various Pitch-to-Diameter Ratios," Trans. ASME, J. Pressure Vessel Technol., Vol. 104, pp. 168-174.
11. Jendrzejczyk, J. A., and S. S. Chen, 1987, "Motion-Dependent Fluid Forces Acting on a Tube Row in Crossflow," In Mechanical Signature Analysis: Machinery Vibration, Flow-Induced Vibration, and Acoustic Noise Analysis, DE-Vol. 7, ASME, New York, pp. 233-242.
12. Chen, S. S., 1975, "Vibration of Nuclear Fuel Bundles," Nucl. Eng. Des., Vol. 35, pp. 399-422.
13. Chen, S. S., S. Zhu, and J. A. Jendrzejczyk, 1993, "Motion-Dependent Fluid Forces Acting on Tube Arrays in Crossflow," ANL-93/15.
14. Chen, S. S., S. Zhu, and J. A. Jendrzejczyk, 1994, "Fluid Damping and Fluid Stiffness of a Tube Row in Crossflow," To be presented at the 1994 ASME PVP Conference, June 20-24, Minneapolis, Minnesota.
15. Chen, S. S., S. Zhu, and Y. Cai, 1994a, "Fluid-Damping-Controlled Instability of Loosely Supported Tube Arrays in Crossflow," To be presented at the 1994 ASME PVP Conference, June 20-24, Minneapolis, Minnesota.
16. Chen, S. S., J. A. Jendrzejczyk, and M. W. Wambsganss, 1985, "Dynamics of Tubes in Fluid with Tube-Baffle Interaction," J. Pressure Vessel Technology, Vol. 107, pp. 7-17.
17. Chen, S. S., S. Zhu, and Y. Cai, 1993, "Experiment on Fluidelastic Instability of Loosely Supported Tube Arrays in Crossflow," ANL-93/16.
18. Chen, S. S., S. Zhu, and Y. Cai, 1994b, "An Unsteady Flow Theory for Vortex-Induced Vibration," Submitted for publication.
19. Cai, Y., and S. S. Chen, 1993, "Non-Linear Dynamics of Loosely Supported Tubes in Crossflow," J. Sound Vib., Vol. 168(3), pp. 449-468.
20. Chen, S. H., and S. S. Chen, 1993a, "Nonlinear Fluid-Stiffness-Controlled Instability of Tube Row in Crossflow," Presented at Asia-Pacific Vibration Conference, November 14-18, 1993, Kitakyushu, Japan; Proc. of Symp. on Flow-Induced Vibrations in Engineering Systems, Vol. 1, pp. 8-13.
21. Chen, S. H., and S. S. Chen, 1993b, "Chaotic Vibration in Fluidelastic Instability of a Tube Row in Crossflow," ASME Publication PVP-Vol. 258, pp. 11-19.

DATE
FILMED
6/1/94
END